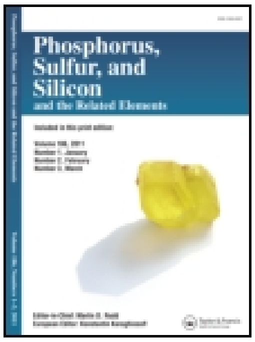

Phosphorus, Sulfur, and Silicon and the Related Elements

ISSN: 1042-6507 (Print) 1563-5325 (Online) Journal homepage: http://www.tandfonline.com/loi/gpss20

Novel Aryl Substituted Silanes Part I: Synthesis and Characterization of Diaryl Silicon Dichlorides

Judith Binder, Roland C. Fischer, Michaela Flock, Ana Torvisco & Frank Uhlig

To cite this article: Judith Binder, Roland C. Fischer, Michaela Flock, Ana Torvisco & Frank Uhlig (2015) Novel Aryl Substituted Silanes Part I: Synthesis and Characterization of Diaryl Silicon Dichlorides, Phosphorus, Sulfur, and Silicon and the Related Elements, 190:11, 1980-1993, DOI: 10.1080/10426507.2015.1049744

To link to this article: http://dx.doi.org/10.1080/10426507.2015.1049744

Phosphorus, Sulfur, and Silicon, 190:1980–1994, 2015

ISSN: 1042-6507 print / 1563-5325 online
DOI: 10.1080/10426507.2015.1049744

NOVEL ARYL SUBSTITUTED SILANES PART I: SYNTHESIS AND CHARACTERIZATION OF DIARYL SILICON DICHLORIDES

Judith Binder, Roland C. Fischer, Michaela Flock, Ana Torvisco, and Frank Uhlig
Institut für Anorganische Chemie, TU Graz, Graz, Austria

GRAPHICAL ABSTRACT

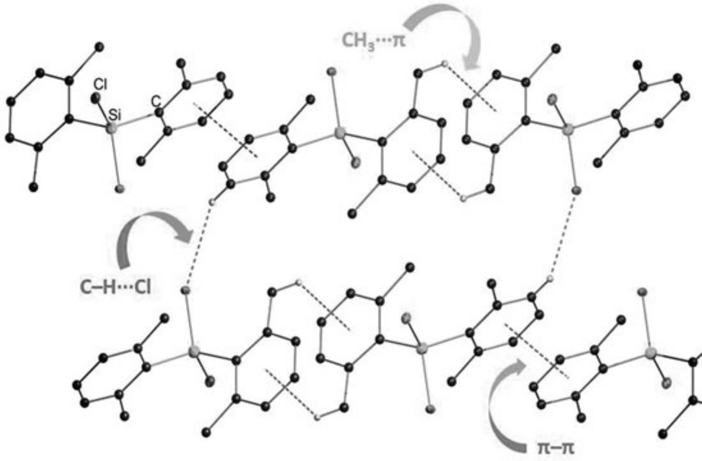

Abstract *A series of novel and previously published silicon dichlorides,* R_2SiCl_2 *(R = benzyl, fluorenyl, p-tolyl p-n-butyl, p-biphenyl, m-tolyl, o-tolyl, 2,4-xylyl, 2,6-xylyl, p-biphenyl, 1-naphthyl, 9-anthracenyl), were synthesized and characterized using* ^{1}H-, ^{13}C- *and* ^{29}Si *NMR spectroscopy. Effects of substituent bulk on both experimental and calculated* ^{29}Si *NMR shifts are compared between reported silicon dichlorides species and novel dichlorides herein. In addition, single crystal X-ray diffraction was employed to elucidate the molecular structure of all solid diorgano silicon dichlorides. These compounds display non-covalent intermolecular interactions in the form of edge to face,* π–π *stacking, and* $CH_3\cdots\pi$ *interactions. Dependency of substituent type on the nature of interactions present will be highlighted and discussed.*

Keywords Diaryl silicon dichlorides; ^{29}Si NMR; solid state structures; intermolecular interactions

Received 24 March 2015; accepted 5 May 2015.

Address correspondence to Judith Binder and Frank Uhlig, Institut für Anorganische Chemie, TU Graz, Stremayrgasse 9/IV, Room CE04502, 8010 Graz, Austria. E-mail: j.binder@tugraz.at; frank.uhlig@tugraz.at

Color versions of one or more of the figures in the article can be found online at www.tandfonline.com/gpss.

INTRODUCTION

Organosilicon halides are one of the most important groups of functional organosilanes and, through a vast variety of substitution reactions, are versatile precursors to diverse organosilicon derivatives.[1] Diorgano dichlorosilanes are also the most popular precursor compounds to create functionalized oligo- and polyorganosilanes.[1] Oligo- as well as polysilanes, with their unbroken chains of catenated silicon atoms, are the prototypical-conjugated systems. They can be regarded as one-dimensional analogs to elemental silicon, on which, of course, nearly all of modern electronics is based. Delocalization of the σ-electrons in the Si–Si bonds gives the polysilanes unique optoelectronic properties[2] that have already led to recent applications concerning the high room temperature luminescence.[3] Due to the high affinity of silicon to oxygen, the silicon halides are usually easily hydrolyzed by water or alcohols, leading to the corresponding (poly-)silanols. The chemistry of polysilanols is extensive and is of particular importance in the silicone polymer industry and sol gel processing, though there is also a growing interest in other applications, like anion-recognition by silanediol-based receptors[4–6] or silanediol protease inhibitors.[7,8] In addition, treatment of organochlorosilanes with $LiAlH_4$ leads to hydrogen rich silanes, which have shown to serve as important substrates for many applications, such as the single-source precursors in CVD processes, as monomeric substrates for sigma-bond metathesis and hydrosilylation, as well as ligands for transition metal catalysts. Furthermore, hydrogen rich silanes are used to generate polysilanes via dehydrogenative coupling.[9–12]

Despite recent interests in arylchlorosilane chemistry, there is a considerable lack of experimental data. For instance, ^{29}Si NMR spectroscopy was established in the early sixties,[13] but did not become conventional until the late eighties. Consequently, despite many compounds being presented in literature, ^{29}Si NMR shifts are not reported and there is no information on effects of the bulk of the aryl substituent on NMR behavior. In addition, only a few crystal structures of dichlorosilanes have been published thus far;[14–17] therefore, there is little information on how the substituent affects the solid state structures of these compounds. In particular, the presence of stabilizing factors in the form of non-covalent secondary interactions including $\pi-\pi$ stacking, edge to face, or $CH_3\cdots\pi$ interactions attributed to the nature of the aromatic substituents in the solid state has not been reported.

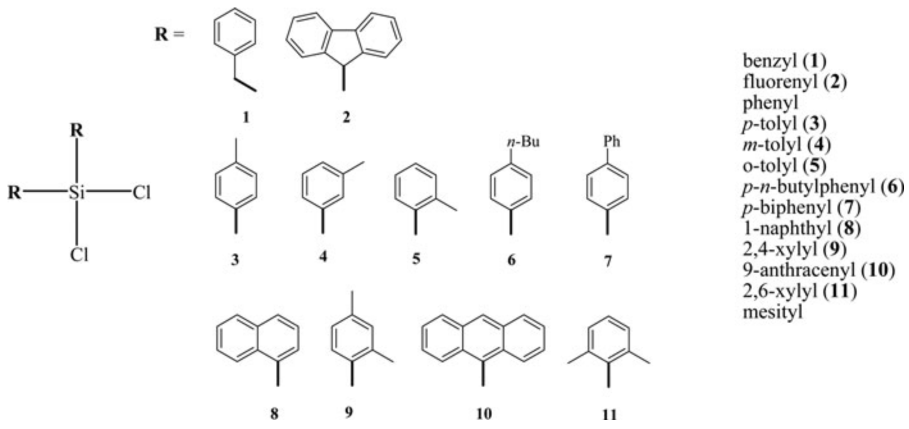

Figure 1 Target molecules. ^{29}Si NMR shifts published for compounds R = phenyl[18] and R = mesityl.[19]

For this reason, novel and previously published organosilicon dichlorides have been synthesized in which the silicon atom is bonded to either an *sp*^{3} carbon (Figure 1, Compounds 1 and 2) or bonded directly to an *sp*^{2} carbon of an aromatic system (Figure 1, Compounds 3–11) with increasing steric demand of the substituent. ^{29}Si NMR spectroscopy supplemented by DFT calculations was performed and the effect of substituent bulk on shifts was examined for all novel species and for published compounds where ^{29}Si NMR data had not been reported. Solid state structures of presented compounds display intermolecular interactions and are highlighted and discussed.

RESULTS AND DISCUSSION

Synthesis

For both novel and previously synthesized dichlorides (Figure 1) presented, a lithiation reaction (General Procedure A) was preferred over published procedures.[20–22] In a typical experiment, the aryl/alkyl bromide was reacted with *n*-BuLi at −78°C in Et_2O (Scheme 1). The solution was transferred via cannula to $SiCl_4$, in ether, cooled to 0°C. Salt formation was observed and the reaction stirred.

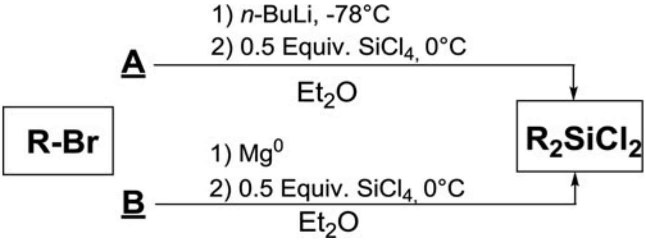

Scheme 1 General synthetic procedures A and B towards silicon dichlorides. R = benzyl (**1**), fluorenyl (**2**), *p*-tolyl (**3**), *m*-tolyl (**4**), *o*-tolyl (**5**), *p*-*n*-butylphenyl (**6**), *p*-biphenyl (**7**), 1-naphthyl (**8**), 2,4-xylyl (**9**), 9-anthrachenyl (**10**), 2,6-xylyl (**11**).

In the case of the fluorenyl substituent, lithiation of the aryl bromide did not result in the desired compound but rather formation of product mixtures including fluorene. However, direct lithiation of fluorene at 0°C resulted in formation of pure $fluorenyl_2SiCl_2$ (**2**). 9-$Anthracenyl_2SiCl_2$ (**10**) was prepared similar to literature;[23] however, despite several attempts, the pure compound could not be isolated. Compound **10** was purified by sublimation to remove anthracene as a major byproduct, which led to a melting point of 161–162°C, which is notably higher than the one presented in literature, reported at 128°C.[23]

Due to availability of the appropriate Grignard for compounds *p*-*n*-$butylphenyl_2SiCl_2$ (**6**) and *p*-$biphenyl_2SiCl_2$ (**7**), a Grignard reaction was used for compound formation. In this route, the Grignard was added to a solution of $SiCl_4$ in Et_2O cooled to 0°C. The reaction was stirred for 4 h and allowed to warm to room temperature. Et_2O was removed and the resulting residue was redissolved in hot toluene. Insoluble salts were removed via filtration and washed with hot toluene.

To obtain $benzyl_2SiCl_2$ (1) general procedure B was used. As already stated in earlier publications, preparation of the dichlorosilane using benzyllithium leads mainly to the coupling product dibenzyl. This is caused by the reactivity of benzyllithium and the ease with which benzyl halides undergo displacement of the halide ion by organometallic

Table 1 Experimental and M06L/Iglo-II calculated ^{29}Si NMR shifts of diorgano dichlorosilanes in C_6D_6. calc = calculated; exp = experimental

$R_2SiCl_{2R} =$	$^{29}Si_{exp}$ [ppm]	$^{29}Si_{calc}$ [ppm]
Benzyl	22.72	26.7
Fluorenyl	17.33	22.3
Phenyl[18]	6.20	8.7
p-Tolyl	6.65	8.7
m-Tolyl	6.37	9.6
3,5-Xylyl[25]	Not reported	9.2
o-Tolyl	6.57	10.0
p-*n*-Butylphenyl	6.49	7.8
p-Biphenyl	6.24	7.8
1-Naphthyl	7.58	11.6
2,4-Xylyl	7.23	11.0
9-Anthracenyl	3.02	8.4
2,6-Xylyl	2.08	7.6
Mesityl[19]	4.30	7.5

compounds.[24] For all solid compounds, recrystallization from toluene, pentane, or Et_2O afforded crystals suitable for single crystal X-ray diffraction studies. In some cases, compounds were first purified via distillation under reduced pressure to remove mono- or trisubstituted byproducts (benzyl, *o*-tolyl, 2,4-xylyl, 2,6-xylyl).

^{29}Si NMR: Experimental and Calculated Data

^{29}Si NMR measurements were performed with relaxation delay times ranging from 25 to 60 sec, with the sterically hindered compound 9-anthracenyl$_2$SiCl$_2$ (**10**) requiring the longest delay (Table 1). For compounds bearing a proton in position *ortho* to the silicon, population transfer pulse programs such as DEPT were used for measurement.

Benzyl$_2$SiCl$_2$ (**1**) exhibits the largest low field shift in the row of presented compounds followed by the cyclopentadienyl-like fluorenyl$_2$SiCl$_2$ (**2**). As expected, when silicon is bonded to an *sp*^{2} hybridized carbon these are shifted to higher fields compared to usual silicon organic variety with an *sp*^{3} hybridized carbon. 1-Naphthyl$_2$SiCl$_2$ (**8**) with only one proton in β-position of the rather planar naphthyl group shows a slightly downfield shift compared to the phenyl derivatives with a substituent in the *para* position. The substitution on the phenyl ring with a methyl group in *ortho*-, *meta*-, or *para*-position does

Table 2 Selected bond lengths and angles for presented silicon dichlorides

	Space group	Si–C (Å)(avg.)	Si–Cl (Å)(avg.)	C–Si–C (°)	Cl–Si–Cl (°)
Benzyl$_2$SiCl$_2$ (**1**)	P2$_1$/n	1.857(3)	2.081(2)	113.53(1)	107.04(4)
Fluorenyl$_2$SiCl$_2$ (**2**)	P-1	1.878(4)	2.059(4)	117.65(5)	105.01(2)
o-Tolyl$_2$SiCl$_2$ (**5**)	P2$_1$/c	1.858(3)	2.065(3)	116.94(2)	104.79(5)
1-Naphthyl$_2$SiCl$_2$ (**8**)	P2$_1$/n	1.859(3)	2.063(2)	116.84(10)	106.18(4)
2,4-Xylyl$_2$SiCl$_2$ (**9**)	P-1	1.858(3)	2.059(2)	118.15(9)	104.95(4)
2,6-Xylyl$_2$SiCl$_2$ (**11**)	P-1	1.877(2)	2.069(2)	113.72(7)	102.66(3)
Mesityl$_2$SiCl$_2$ [16]	P-1	1.875(2)	2.064(2)	113.42(8)	102.96(4)

Table 3 List of non-covalent interactions for presented silicon dichlorides; d = distance between planes (Å), R = offset

	π–π Stacking (Å)				
	d	R	Edge to face (Å)	$CH_3 \cdots \pi$ (Å)	C–H···Cl (Å)
Benzyl$_2$SiCl$_2$ (**1**)			3.13	3.14	
Fluorenyl$_2$SiCl$_2$ (**2**)	3.353.53	0.961.23			2.84
o-Tolyl$_2$SiCl$_2$ (**5**)			2.69 − 3.07		
1-Naphthyl$_2$SiCl$_2$ (**8**)	3.583.60	1.541.23	2.95		2.91
2,4-Xylyl$_2$SiCl$_2$ (**9**)			3.26	2.99	
2,6-Xylyl$_2$SiCl$_2$ (**11**)	3.45	1.46		3.24	2.99

not show a clear trend, but all exhibit a similar shift in the range of 6.5 ppm. Unexpectedly, 2,4-xylyl$_2$SiCl$_2$ (**9**) shows a slight downfield shift compared to the *meta*-substituted phenyl. Introduction of a second group in the *ortho* position as in 2,6-xylyl$_2$SiCl$_2$ (**11**) and mesityl$_2$SiCl$_2$ or 9-anthracenyl$_2$SiCl$_2$ (**10**) leads to increased shielding towards silicon, expressed by a notably high field shift. The DFT calculated ^{29}Si NMR chemical shifts are

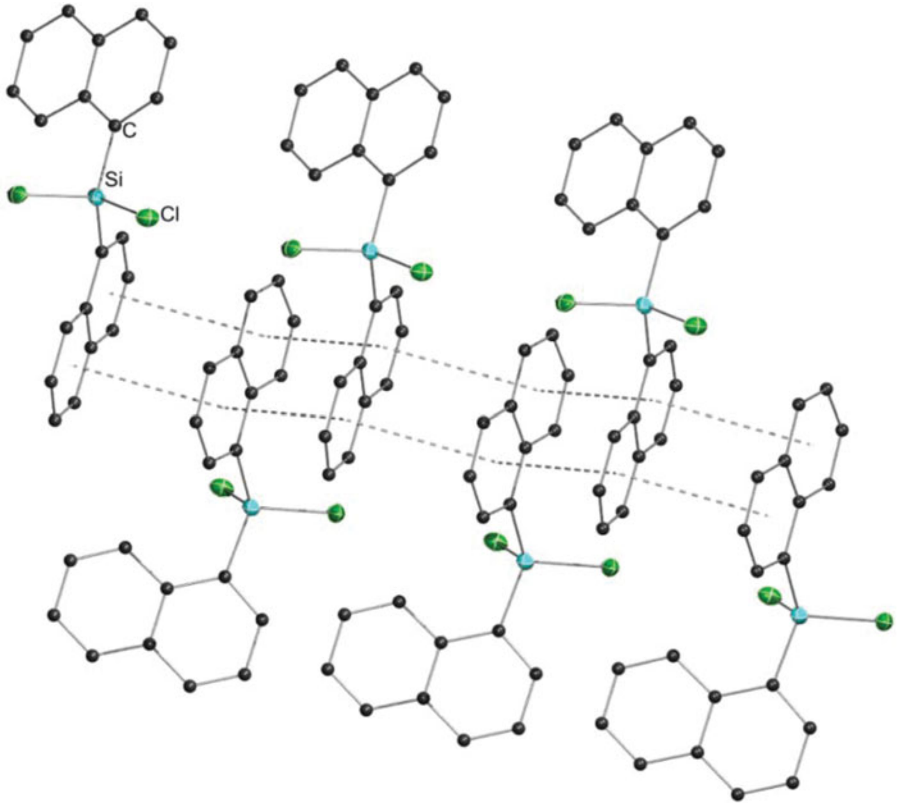

Figure 2 Crystal packing diagram for 1-naphthyl$_2$SiCl$_2$ (**8**). $\pi-\pi$ stacking interactions highlighted by dashed bonds. All non-carbon atoms shown as 30% shaded ellipsoids. All hydrogen atoms, edge to face and C−H···Cl interactions removed for clarity.

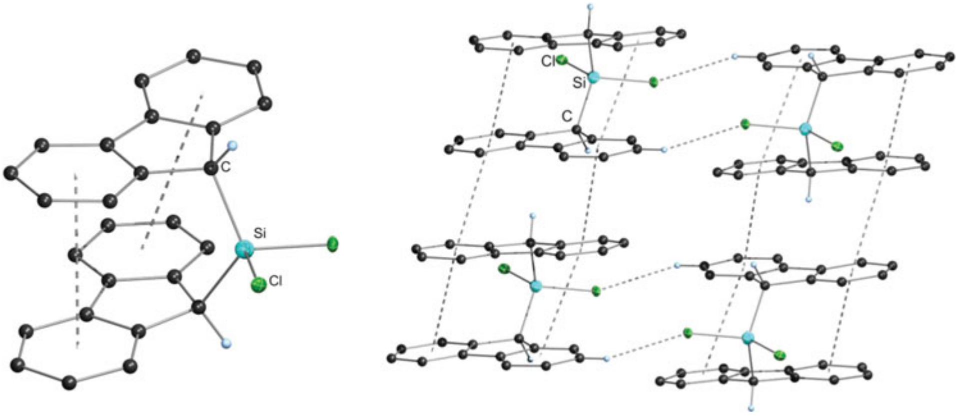

Figure 3 Crystal structure and crystal packing diagram of fluorenyl$_2$SiCl$_2$ (**2**). All non-carbon atoms shown as 30% shaded ellipsoids. All hydrogen atoms except the hydrogen on the methylene carbon on the fluorenyl substituent and not involved in intermolecular interactions removed for clarity. $\pi-\pi$ stacking and C−H···Cl interactions highlighted by dashed bonds. All non-carbon atoms shown as 30% shaded ellipsoids.

all only +2 ppm to +5.4 ppm higher than the observed peaks. This agreement between measured and DFT calculated ^{29}Si NMR chemical shifts is exceptionally good with the maximum deviation of +5.4 ppm in the case of the 9-anthracenyl substituted compound **10.**

X-Ray Crystallography

Solid state structures of compounds **1**, **2**, **5**, **8**, **9**, **11** were obtained through recrystallization of powders obtained. Despite several attempts, X-ray quality crystals of anthracenyl$_2$SiCl$_2$ (**10**) could not be isolated. In each case, the silicon atom is found in a

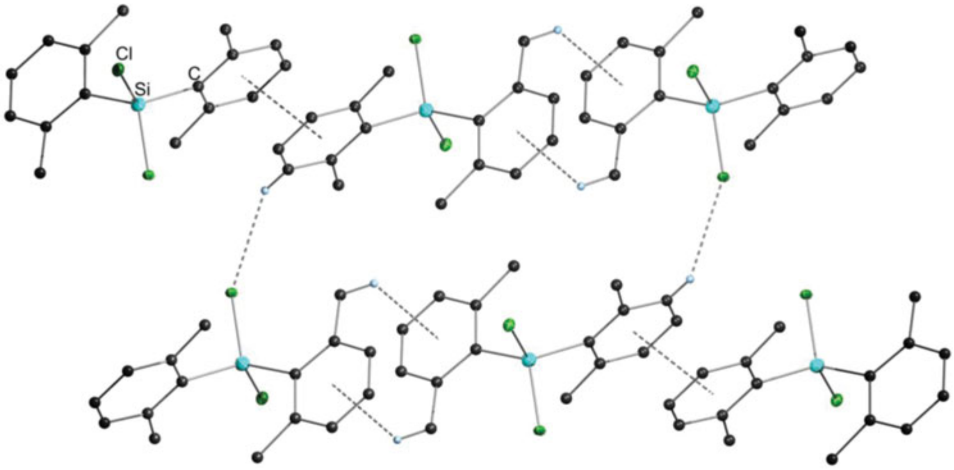

Figure 4 Crystal packing diagram for 2,6-xylyl$_2$SiCl$_2$ (**11**). CH$_3$···π and C−H···Cl interactions highlighted by dashed bonds. All non-carbon atoms shown as 30% shaded ellipsoids. Hydrogen atoms not involved in intermolecular interactions removed for clarity.

distorted tetrahedral environment bound to two chlorine atoms and two substituents. Table 2 summarizes average bond lengths and angles for presented compounds and comparable silicon dichlorides.

With respect to averaged Si–C and Si–Cl bond lengths, these fall within a narrow range of 1.86–1.88 and 2.06–2.08 Å respectively (Table 2), and are seemingly not affected by the degree of bulkiness afforded by the organic substituent on silicon. Due to the higher electronegativity of the chlorine substituent versus the aryl substituent, Cl–Si–Cl angles are more narrow than the C–Si–C angles due to Bent's rule.[26] However, the position of methyl substitution on the aryl ring also seems to have an influence on the C–Si–C and Cl–Si–Cl angles; depending on the position of methyl substitution on the aryl ring, the angles around the silicon atom are varying considerably. Both *o*-tolyl$_2$SiCl$_2$ (**5**) and 2,4-xylyl$_2$SiCl$_2$ (**9**) display Cl–Si–Cl angles of 104.79(5)° and 104.95(4)° respectively, while the additional methyl group in the aryl moiety of 2,6-xylyl$_2$SiCl$_2$ (**11**) (102.66(3)°) and mesityl$_2$SiCl$_2$ (102.96(4)°) results in more narrow angles. This is a direct result of increased steric repulsion from substituents on the *ortho* position of the aryl moiety on the chlorine atoms. In addition, the C–Si–C angles in 2,6-xylyl$_2$SiCl$_2$ (**11**) (113.72(7)°) and mesityl$_2$SiCl$_2$ (113.42(8)°) are much narrower than seen for the other presented dichlorides coinciding with the aforementioned added steric demand of the methyl groups on the 2- and 6-position on the chlorine atoms. This added stress is not seen in 1-naphthyl$_2$SiCl$_2$ (**8**), which displays a wider Cl–Si–Cl (106.18(4)°) and a C–Si–C angle (116.84(10)°) similar to that of *o*-tolyl$_2$SiCl$_2$ (**5**).

While the molecular structure of these aryl silicon dichlorides is unexceptional, the extended solid state structure of these compounds displays noteworthy aromatic secondary interactions. Specifically, interactions attributed to the nature of the aromatic substituents including $\pi-\pi$ stacking, edge to face, or $CH_3\cdots\pi$ interactions are present. These stabilizing factors have been rarely discussed for silicon dichloride species in the solid state due to lack of representative examples. All aromatic non-covalent interactions present in the dichloride species included in this publication are within acceptable ranges found in biological and organic systems[27–29] and are similar to those found for a series of aryl substituted tin halides and hydrides.[30, 31] These stabilizing interactions are described and compared to those present in previously reported species (Table 3). In addition, several of these compounds exhibit close $C-H\cdots Cl$ interactions ranging from 2.84 to 2.99 Å.

1-Naphthyl$_2$SiCl$_2$ (**8**) (Figure 2) shows a $\pi-\pi$ stacking conformation in the solid state, where the molecules are arranged in a way to maximize these interactions creating infinite columns of parallel stacked planar naphthyl derivatives with a specific distance (d = 3.58 and 3.60 Å) between the ring centers. They are also found to be parallel-displaced to each other with a certain off-set (R = 1.54 and 1.23; Table 3). These values are in accordance to reported ranges of 3.4−3.6 Å for benzene[28] or 3.35 Å in graphite[32] and has been described for related aryl tin species.[30,31] $\pi-\pi$ stacking interactions are also observed for 2,6-xylyl$_2$SiCl$_2$ (**11**) (d = 3.45 Å, R = 1.46).

The planar fluorenyl substituents in the molecular structure of fluorenyl$_2$SiCl$_2$ (**2**) (Figure 3) adopt a parallel orientation, which also allows for the presence of intramolecular $\pi-\pi$ stacking (d = 3.35 Å, R = 0.96). The stacked fluorenyls then interact with a neighboring molecule through more $\pi-\pi$ stacking (d = 3.53 Å, R = 1.23) resulting in π-stacked oligomeric chains (Figure 3). Similar solid state interactions have been described for compounds resulting from the anionic initialized polymerization of dibenzofulvene[33] and similar $\pi-\pi$ stacking distances are also observed in the molecular structures of silicon fluorenyl derivatives.[34, 35]

Table 4 Crystallographic data and details of measurements for compounds 1, 2 and 5, 8, 9, 11

Compound	$Benzyl_2SiCl_2$ (1)	$Fluorenyl_2SiCl_2$ (2)	*o*-$Tolyl_2SiCl_2$ (5)	1-$Naphthyl_2SiCl_2$ (8)	2,4-$Xylyl_2SiCl_2$ (9)	2,6-$Xylyl_2SiCl_2$ (11)
Formula	$C_{14}H_{14}Cl_2Si$	$C_{26}H_{18}Cl_2Si$	$C_{14}H_{14}Cl_2Si$	$C_{20}H_{14}Cl_2Si$	$C_{16}H_{18}Cl_2Si$	$C_{16}H_{18}Cl_2Si$
Fw (g mol^{-1})	281.24	429.39	281.24	353.30	309.29	309.29
a (Å)	9.8244(2)	7.4007(2)	6.9270(4)	15.1186(4)	7.9627(3)	8.5365(3)
b (Å)	13.8493(4)	9.6653(3)	15.1723(8)	7.3181(2)	8.1319(3)	8.6184(3)
c (Å)	10.5055(3)	14.8304(5)	13.3144(7)	15.7994(4)	12.6224(4)	10.7234(4)
α (°)	90	96.9000(12)	90	90	105.372(1)	80.4680(18)
β (°)	102.997(1)	103.4840(12)	97.305(2)	110.894(1)	94.096(2)	82.8440(19)
γ (°)	90	104.4250(13)	90	90	96.305(2)	81.8820(19)
V (Å^3)	1392.77(6)	981.00(5)	1387.97(13)	1633.09(7)	779.00(5)	766.09(5)
Z	4	2	4	4	2	2
Crystal size (mm)	0.13 × 0.12 × 0.10	0.20 × 0.19 × 0.10	0.42 × 0.18 × 0.16	0.30 × 0.10 × 0.09	0.16 × 0.09 × 0.08	0.12 × 0.11 × 0.05
Crystal habit	Block, colorless	Block, colorless	Block, colorless	Block, colorless	Block, colorless	Block, colorless
Crystal system	Monoclinic	Triclinic	Monoclinic	Monoclinic	Triclinic	Triclinic
Space group	$P2_1/n$	P-1	$P2_1/c$	$P2_1/n$	P-1	P-1
d_{calc} (mg/m^3)	1.341	1.454	1.346	1.437	1.319	1.341
μ (mm^{-1})	0.53	0.40	0.53	0.47	0.48	0.49
T (K)	100(2)	100(2)	100(2)	100(2)	100(2)	100(2)
2θ range (°)	2.5–27.1	2.2–27.1	2.0–30.1	2.9–27.1	1.0–25.0	2.9–27.1
F(000)	584	444	584	728	324	324
R_{int}	0.082	0.019	0.033	0.104	0.036	0.029
Independent reflns	2428	4329	4070	3556	2723	3373
No. of params	154	262	156	208	176	176
R1, wR2 (all data)	R1 = 0.0458 wR2 = 0.1208	R1 = 0.0264 wR2 = 0.0696	R1 = 0.0618 wR2 = 0.1736	R1 = 0.0582 wR2 = 0.1285	R1 = 0.0439 wR2 = 0.0826	R1 = 0.0409 wR2 = 0.0727
R1, wR2 (>2σ)	R1 = 0.0423 wR2 = 0.1166	R1 = 0.0250 wR2 = 0.0685	R1 = 0.0590 wR2 = 0.1724	R1 = 0.0472 wR2 = 0.1191	R1 = 0.0377 wR2 = 0.0798	R1 = 0.0308 wR2 = 0.0682

Mo Kα ($\lambda = 0.71073$Å). $R_1 = \Sigma/\,|F_o|\text{-}\,|F_c|/|\Sigma|F_d$; wR2 = $[\Sigma_w(F_o{}^2\text{-}F_2{}^2)^2/\Sigma_w(F_o{}^2)^2]^{1/2}$.

While edge to face interactions are exclusively present in the extended solid state structure of *o*-tolyl$_2$SiCl$_2$ (**7**) (2.69−3.07 Å) consistent with the availability of phenyl hydrogens, they are also seen in benzyl$_2$SiCl$_2$ (**1**), 2,4-xylyl$_2$SiCl$_2$ (**9**), and 1-naphthyl$_2$SiCl$_2$ (**8**) (Table 3). The addition of a methyl group onto the aryl substituent of 2,4-xylyl$_2$SiCl$_2$ (**9**) results in $CH_3 \cdots \pi$ interactions (2.99 Å) through the methyl in the 4-position. Methyl addition at the 6-position in 2,6-xylyl$_2$SiCl$_2$ (**11**) results in infinite chains propagated through both $\pi - \pi$ stacking (d = 3.45 Å, R = 1.46) and $CH_3 \cdots \pi$ interactions (3.24 Å; Figure 4). In the benzyl$_2$SiCl$_2$ (**1**) species, neighboring molecules orient so as to maximize $CH_3 \cdots \pi$ interactions from one of the methanide (CH_2−Ph) hydrogens with the phenyl substituent of the other compound (3.14 Å).

CONCLUSION

A series of dichloro silanes was synthesized via two general reaction pathways and characterized through single crystal X-ray diffraction. In all cases, crystallographic analysis in the extended solid state structures of these compounds reveals highly interesting structural motifs displaying a dependency of the secondary interactions that arise as a consequence of the nature of the substituent on silicon. Both experimentally obtained and DFT M06L/Iglo-II/mPW1PW91/6-31+G* calculated ^{29}Si NMR shifts agree exceptionally well with absolute deviations between +2 and +7 ppm. The obtained compounds provide promising starting materials for novel polymers as well as for further reactions.

EXPERIMENTAL

Materials and Methods

All reactions, unless otherwise stated, were carried out using standard Schlenk line techniques under nitrogen atmosphere, using oven-dried glassware. All dried and deoxygenated solvents were obtained from a solvent drying system (Innovative Technology Inc.). C_6D_6 was distilled over sodium and stored under nitrogen. $SiCl_4$ was purchased from ABCR and distilled before use. All other chemicals from commercial sources were utilized without further purification. Melting point measurements were carried out by three-fold determination with a Stuart Scientific SMP 10 (up to 300°C). Degassed H_2SO_4 (10%) was diluted with deionized water. GC-MS measurements were performed on an Agilent Technologies GC system (column: HP-5MS) with mass selective detector Type Agilent 5975C using EI at 70 eV.

NMR Spectroscopy

^{1}H (300.22 MHz), ^{13}C (75.5 MHz), and ^{29}Si (59.64 MHz) NMR spectra were recorded on a Mercury 300 MHz spectrometer from Varian at 25°C. Chemical shifts for ^{1}H, ^{13}C, and ^{29}Si were recorded in parts per million with either TMS (0.00 ppm), $CDCl_3$ (7.26 ppm for ^{1}H or 77.0 ppm for ^{13}C), or C_6D_6 (7.16 ppm for ^{1}H or 128.0 ppm for ^{13}C) as a reference. Coupling constants (*J*) are reported in Hertz (Hz).

Crystal Structure Determination

All crystals suitable for single crystal X-ray diffractometry were removed from a Schlenk flask and immediately covered with a layer of silicone oil. A single crystal was selected, mounted on a glass rod on a copper pin, and placed in the cold N_2 stream provided by an Oxford Cryosystems cryostream. XRD data collection was performed on a Bruker APEX II diffractometer with use of Mo Kα radiation (λ = 0.71073 Å) and a CCD area detector. Empirical absorption corrections were applied using SADABS.[36] The structures were solved with use of either direct methods or the Patterson option in SHELXS and refined by the full-matrix least-squares procedures in SHELXL.[37,38] The space group assignments and structural solutions were evaluated using PLATON.[39,40] Non-hydrogen atoms were refined anisotropically. All other hydrogen atoms were located in calculated positions corresponding to standard bond lengths and angles. Intermolecular interactions for presented and published compounds were determined by the calculation of centroids and planes feature of the programs Mercury[41] and Diamond.[42] Table 4 contains crystallographic data and details of measurements and refinement for compounds **1**, **2** and **5**, **8**, **9**, **11**. (CCDC 1053138–1053143). CCDC 1053138–1053143 contain the supplementary crystallographic data for presented compounds, respectively. These data can be obtained free of charge from The Cambridge Crystallographic Data Centre via www.ccdc.cam.ac.uk/data_request/cif.

Computational Details

All calculations have been carried out using the Gaussian09 program package[43] on a computing cluster with blade architecture. The mPW1PW91 hybrid functional[44] has been used together with the 6-31+G* basis sets for geometry optimizations and vibrational frequency calculations. Magnetic shieldings have been obtained using the M06L functional[45] in combination with IGLO-II basis sets.[46] The magnetic shielding of tetramethylsilane (σ(Si) = 372.7 ppm) obtained at the same level of theory was used as reference for calculating ^{29}Si NMR chemical shifts.

Synthesis

General Procedure A for R_2SiCl_2: Compounds 2–5 and 8–11. A flask furnished with a dropping funnel was charged with the aryl/alkylbromide in Et_2O. *n*-BuLi (1.6 M in hexane) diluted with Et_2O was added dropwise at −78°C. After addition, the reaction was kept at −78°C for 10 min and was then allowed to warm to room temperature and stirred for 30 min. The solution was transferred via cannula to $SiCl_4$ dissolved in Et_2O at 0°C. The reaction was stirred for 2 h and was allowed to warm to room temperature. The solvent was removed under reduced pressure and the residue dissolved in boiling toluene. Insoluble salts were removed via filtration through cellite and washed with hot toluene. The solvent from the resulting clear solution was removed under reduced pressure, followed by purification via distillation or recrystallization.

Fluorenyl$_2$SiCl$_2$ (2). Fluorene (0.94 g, 5.5 mmol) was dissolved in Et_2O (20 mL). The solution was cooled to 0°C and *n*-BuLi (3.6 mL 1.6 M in hexane, 5.7 mmol, 1.1 equiv.) was added dropwise via syringe. The resulting orange solution was stirred for 1 h at room temperature. Completeness of lithiation was monitored by ^{1}H NMR. Et_2O (20 mL) was added to the solution followed by slow addition of $SiCl_4$ (0.314 mL, 2.76 mmol, 0.5 equiv.) at 0°C. The resulting cloudy yellow solution was stirred for 4 h. Et_2O was removed under reduced pressure and the residue dissolved in boiling toluene. Insoluble salts were removed via filtration through cellite and washed with hot toluene. The resulting clear solution was concentrated under reduced pressure. Crystals suitable for X-ray diffraction analysis were grown at room temperature. Yield 60% (0.71 g, 1.6 mmol), mp = 173°C. ^{1}H NMR (300 MHz, $CDCl_3$) δ 7.58 (d, $J = 7.6$ Hz, 1H), 7.45 (d, $J = 7.7$ Hz, 1H), 7.25 (t, $J = 7.5$ Hz, 2H), 7.07 (t, $J = 7.5$ Hz, 1H), 4.16 (s, 1H). ^{13}C NMR (75.5 MHz, $CDCl_3$) δ 141.4, 139.9, 126.9, 126.4, 125.2, 120.2, 43.0 ppm. ^{29}Si NMR (59.64 MHz, C_6D_6): δ 17.33 ppm. MS (70 eV, *m/z*) = 428 (M^+).

p-Tolyl$_2$SiCl$_2$ (3). 4-Bromotoluene (17.5 mL, 142 mmol, 1 equiv.) in Et_2O (150 mL). Addition of *n*-BuLi (97.76 mL 1.6 M in hexane, 156 mmol, 1.1 equiv.). $SiCl_4$ (8.16 mL, 71 mmol, 0.5 equiv.) in Et_2O (100 mL). Purification by distillation. Yield 62% (12.4 g, 44 mmol) of colorless liquid. bp (obs.) = 110–112°C (0.4 mbar).[20] ^{1}H NMR (300 MHz, C_6D_6): δ 7.67 (d, $J = 7.6$ Hz, 4H), 6.93 (d, $J = 7.5$ Hz, 4H), 2.00 (s, 6H) ppm. ^{13}C NMR (75.5 MHz, C_6D_6): δ 142.2, 134.6, 129.4, 129.2, 21.5 (CH_3) ppm. ^{29}Si NMR (59.64 MHz, C_6D_6): δ 6.65 ppm. MS (70 eV, *m/z*) = 280.1 (M^+).

m-Tolyl$_2$SiCl$_2$ (4). 3-Bromotoluene (99%) (14.27 mL, 83 mmol, 1 equiv.) in Et_2O (100 mL). Addition of *n*-BuLi (56.8 mL, 1.6 M in hexane, 91 mmol, 1.1 equiv.) in Et_2O (20 mL). $SiCl_4$ (4.73 mL, 41 mmol, 0.5 equiv.) in Et_2O (80 mL). Purification by distillation. Yield 36% (4.17 g, 15 mmol) of colorless liquid. bp = 140–143°C (3 mbar).[47] ^{1}H NMR (300 MHz, C_6D_6): δ 7.65 (s, 2H), 7.58 (d, $J = 7.0$ Hz, 2H), 7.10 (t, $J = 7.4$ Hz, 2H), 7.03 (d, $J = 7.2$ Hz, 2H), 2.04 (s, 6H) ppm. ^{13}C NMR (75.5 MHz, C_6D_6): δ 138.8, 134.9, 132.9, 132.3, 131.6, 128.7, 21.5 (CH_3) ppm. ^{29}Si NMR (59.64 MHz, C_6D_6): δ 6.4 ppm. MS (70 eV, *m/z*) = 280.0 (M^+).

o-Tolyl$_2$SiCl$_2$ (5). 2-Bromotoluene (12.8 mL, 106 mmol, 1 equiv.) in Et_2O (150 mL). Addition of *t*-BuLi (73.2 mL, 1.6 M in hexane, 117 mmol, 1.1 equiv.) in Et_2O (20 mL). $SiCl_4$ (6.1 mL, 53 mmol, 0.5 equiv.) in Et_2O (100 mL). Purification by distillation. Crystals suitable for X-ray diffraction analysis were grown from toluene at 4°C. Yield 67% (10.0 g, 36 mmol). mp = 74–75°C. bp (obs.) = 114–116°C (0.4 mbar). ^{1}H NMR (300 MHz, C_6D_6): δ 7.95 (dd, $J = 7.5$, 1.5, 2H), 7.08 (td, $J = 7.5$, 1.5, 2H), 6.98 (td, $J = 7.5$, 0.5, 2H), 6.85 (dd, $J = 7.6$, 0.5, 2H), 2.24 (s, 6H) ppm. ^{13}C NMR (75.5 MHz, C_6D_6): δ 144.0, 135.6, 132.2, 131.3, 131.1, 126.0, 22.8 (CH_3) ppm. ^{29}Si NMR (59.64 MHz, C_6D_6): δ 6.57 ppm. MS (70 eV, *m/z*) = 280.0 (M^+).

1-Naphthyl$_2$SiCl$_2$ (8). 1-Bromonaphthalene (36.56 g, 176.5 mmol, 1 equiv.) in Et_2O (250 mL). Addition of *n*-BuLi (121.34 mL, 1.6 M in hexane, 194.2 mmol, 1.1 equiv.) in Et_2O (70 mL). $SiCl_4$ (10.14 mL, 88.2 mmol, 0.5 equiv.) in Et_2O (200 mL). Crystals suitable for X-ray diffraction analysis could be grown from toluene at room temperature. Yield: 76% (23.7 g, 67 mmol). mp = 138–139°C. ^{1}H NMR (300 MHz, C_6D_6): δ 8.59–8.50 (m, 2H), 8.14 (d, $J = 6.9$, 2H), 7.60 (d, $J = 8.1$, 2H), 7.55–7.47 (m, 2H), 7.14–7.01 (m, 6H) ppm. ^{13}C NMR (75.5 MHz, C_6D_6): δ 136.1, 135.6, 133.7, 133.0, 129.7, 129.1, 127.9, 126.9, 126.1, 124.9 ppm. ^{29}Si NMR (59.64 MHz, C_6D_6): δ 7.58 ppm. MS (70 eV, *m/z*) = 352.1 (M^+).

2,4-Xylyl$_2$SiCl$_2$ (9). 2,4-Xylylbromide (18.1 g, 97.7 mmol, 1 equiv.) in Et_2O (50 mL). Addition of *n*-BuLi (67.17 mL, 1.6M in hexane, 107 mmol, 1.1 equiv.) in Et_2O (40 mL). $SiCl_4$ (5.61 mL, 48.8 mmol, 0.5 equiv.) in Et_2O (70 mL). 2,4-Xylyl$SiCl_3$ could be identified as byproduct and was removed under vacuum (distillation). Yield 46% (6.94 g, 22.5 mmol) of slightly yellow oil. Colorless crystals suitable for X-ray diffraction analysis were grown from the neat solution at 4°C. mp = 60–62°C. ^{1}H NMR (300 MHz, C_6D_6): δ

7.67 (d, $J = 7.7$, 2H), 6.75 (d, $J = 7.7$, 2H), 6.68 (s, 2H), 2.42 (s, 6H), 1.99 (s, 6H) ppm. ^{13}C NMR (75.5 MHz, C_6D_6): δ 143.5, 141.9, 135.4, 131.66, 126.3, 22.4 (CH_3), 20.9 (CH_3) ppm. ^{29}Si NMR (59.64 MHz, C_6D_6): δ 7.23 ppm. MS (70 eV, *m/z*) = 308.1 (M^+).

9-Anthracenyl$_2$SiCl$_2$ (10). 9-Bromoanthracene (6 g, 23 mmol, 1 equiv.) in Et_2O (50 mL) and THF (50 mL). Addition of *n*-BuLi (16 mL, 1.6 M in hexane, 26 mmol, 1.1 equiv.). $SiCl_4$ (1.33 mL, 12 mmol, 0.5 equiv.) in Et_2O (50 mL). Purification by vacuum sublimation at 60°C (0.04 mbar) to remove anthracene as major byproduct. Yield 35% (1.84g, 4.1 mmol) of yellow solid. mp = 161–162°C. ^{1}H NMR (300 MHz, C_6D_6): δ 8.98 (d, $J = 8.9$, 4H), 8.21 (s, 2H), 7.67 (d, $J = 9.0$, 4H), 7.07–6.97 (m, 4H), 6.97–6.84 (m, 4H) ppm.^{13}C NMR (75.5 MHz, C_6D_6): δ 136.5, 134.0, 131.8, 129.7, 128.1, 126.7, 125.3, 119.7 ppm. ^{29}Si NMR (59.64 MHz, C_6D_6): δ 3.02 ppm. MS (70 eV, *m/z*) = 452.03 (M^+).[48]

2,6-Xylyl$_2$SiCl$_2$ (11). 2,6-Xylylbromide (24.0 g, 129 mmol, 1 equiv.) in Et_2O (100 mL). Addition of *n*-BuLi (97.31 mL, 1.6 M in hexane, 155 mmol, 1.2 equiv.) in Et_2O (50 mL). $SiCl_4$ (7.45 mL, 64.9 mmol, 0.5 equiv.) in Et_2O (100 mL). Small amount of 2,6-xylylSiCl$_3$ could be identified as byproduct and was removed under vacuum (distillation). Crystals suitable for X-ray diffraction analysis could be grown from pentane at room temperature. Yield: 73% (14.65 g, 47.3 mmol). mp = 85°C. ^{1}H NMR (300 MHz, C_6D_6): δ 6.97 (t, $J = 7.6$, 2H), 6.75 (d, $J = 7.5$, 4H), 2.42 (s, 12H) ppm. ^{13}C NMR (75.5 MHz, C_6D_6): δ 143.4, 133.9, 131.1, 129.7, 24.5 (CH_3) ppm. ^{29}Si NMR (59.64 MHz, C_6D_6): δ 2.08 ppm. MS (70 eV, *m/z*) = 308.1 (M^+).

General Procedure B for R$_2$SiCl$_2$: Compounds 1, 6, and 7. A flask equipped with a dropping funnel and a reflux condenser was charged with Mg in THF (or Et_2O). The dropping funnel was charged with the arylbromide in THF. After addition of approximately 10% of the aryl bromide to the Mg, the solution was carefully heated to start the reaction. The aryl bromide was subsequently added slowly. After complete addition, the reaction was refluxed for 2–12 h, until complete consumption of magnesium. The content of Grignard reagent was determined by diluting small volume of the solution with deionized water and titration with 1M HCl using phenolphthalein as indicator. The Grignard solution was slowly added to $SiCl_4$ in THF (or Et_2O) at 0°C. The reaction was stirred for 4 h and was allowed to warm up to room temperature. The solvent was removed under reduced pressure and the residue dissolved in boiling toluene. Insoluble salts were removed via filtration through cellite and washed with hot toluene. The solvent of the resulting clear solution was removed under reduced pressure, followed by purification via distillation or recrystallization.

Benzyl$_2$SiCl$_2$ (1). Mg (2.63 g, 108 mmol, 1 equiv.) in Et_2O (100 mL). Addition of benzylbromide (13 mL, 108 mmol, 1 equiv.) in Et_2O (40 mL). 2 h reflux. $SiCl_4$ (6 mL, 52 mmol, 0.5 equiv.) in Et_2O (80 mL). Purification by distillation. Crystals suitable for X-ray diffraction analysis were grown from toluene at 4°C. Yield 38% (5.9 g, 21 mmol). mp = 50–51°C. bp (obs.) = 103–107°C (0.4 mbar).[49] ^{1}H NMR (300 MHz, $CDCl_3$): δ 7.3–7.1 (m, 10H, Ar-H), 2.60 (s, 4H, Si-CH$_2$-Ar) ppm. ^{13}C NMR (75.5 MHz, C_6D_6): δ 134.1, 129.4, 128.8, 126.1, 28.8 (CH_2) ppm. ^{29}Si (59.6 MHz, C_6D_6): δ 22.72 ppm. MS (70 eV, *m/z*) = 280.1 (M^+).

p-n-Butylphenyl$_2$SiCl$_2$ (6). Mg (2.03 g, 83.6 mmol, 1.1 equiv.) in Et_2O (100 mL). Addition of 1-bromo-4-*n*-butylbenzene (13.46 mL, 76.3 mmol, 1 equiv.) in Et_2O (50 mL). $SiCl_4$ (4.38 mL, 38 mmol, 0.5 equiv.) in Et_2O (80 mL). Purification by distillation. Yield 38% (10.5 g, 29 mmol). bp = 193–195°C (0.7 mbar).[3] ^{1}H NMR (300 MHz, C_6D_6): δ 7.83–7.64 (m, 4H), 7.17–6.97 (m, 4H), 2.56–2.33 (m, 4H), 1.57–1.37 (m, 4H), 1.31–1.13 (m, 4H), 0.85 (t, $J = 7.3$, 6H) ppm. ^{13}C NMR (75.5 MHz, $CDCl_3$): 13.9, 22.4, 33.3, 35.8, 128.5, 129.0, 134.1, 147.0 ppm.[50] ^{29}Si NMR (59.64 MHz, C_6D_6): δ 6.49 ppm. MS (70 eV, *m/z*) = 364.1 (M^+).

p-Biphenyl$_2$SiCl$_2$ (7). Mg (2.5 g, 103 mmol, 1.1 equiv.) in Et_2O (80 mL). Addition of 1-bromo-4-phenylbenzene (16.0 mL, 94 mmol, 1 equiv.) in Et_2O (50 mL). $SiCl_4$ (5.37 mL, 47 mmol, 0.5 equiv.) in Et_2O (80 mL). Small amount of *p*-biphenyl $SiCl_3$ could be identified as byproduct and was removed under vacuum (distillation). Yield 53% (10.2 g, 25.2 mmol), mp = 96–98°C. ^{1}H NMR (300 MHz, C_6D_6): δ 7.03–7.15 (m, 5H), 7.35–7.5 (m, 4H) ppm. ^{13}C NMR (75.5 MHz, C_6D_6): δ 145.0, 140.7, 135.1, 130.9, 129.2, 128.3, 127.6, 127.5 ppm. ^{29}Si NMR (C_6D_6, 59.64 MHz): δ 6.24 ppm. MS (70 eV, *m/z*) = 404.1 (M^+).

FUNDING

This work was supported by the NAWI Graz project, collaboration between the Graz University of Technology and the Graz University.

SUPPLEMENTARY MATERIALS

Supplementary crystallographic data: CCDC 1053138–1053143 contain the supplementary crystallographic data for this article. These data can be obtained free of charge from The Cambridge Crystallographic Data Centre via www.ccdc.cam.ac.uk/data_request/cif.

Supplementary data: Supplementary data related to this article (Figures S1–S3 and DFT calculations) can be found online on the publisher's website at http://dx.doi.org/10.1080/10426507.2015.1049744.

REFERENCES

1. Herzog, U. *The Chemistry of Organic Silicon Compounds*, Vol. 3; John Wiley: Chichester, 2003; pp. 469-489.
2. West, R. *The Chemistry of Organic Silicon Compounds*, Vol. 3; John Wiley: Chichester, 2003; pp. 541-563.
3. Acharya, A.; Seki, S.; Koizumi, Y.; Saeki, A.; Tagawa, S. *J. Phys. Chem. B* **2005,** 109, 20174-20179.
4. Lickiss, P. D. *The Chemistry of Organic Silicon Compounds*, Vol. 4; John Wiley: Chichester, **2003;** pp. 695-744.
5. Kondo, S.; Bie, Y.; Yamamura, M. *Org. Lett.* **2013,** 15, 520-523.
6. Kondo, S.; Harada, T.; Tanaka, R.; Unno, M. *Org. Lett.* **2006,** 8, 4621-4624.
7. Mutahi, M. W.; Nittoli, T.; Guo, L.; Sieburth, S. M. *J. Am. Chem. Soc.* **2002,** 124, 7363-7375.
8. Sieburth, S. M.; Nittoli, T.; Mutahi, A. M.; Guo, L. *Angew. Chem., Int. Ed.* **1998,** 37, 812-814.
9. Harrod, J. F. *Coord. Chem. Rev.* **2000,** 206-207, 493-531.
10. Minge, O.; Nogai, S.; Schmidbaur, H. Z. *Naturforsch., B: Chem. Sci.* **2004,** 59, 153-160.
11. Corey, J. Y. *Chem. Rev.* **2011,** 111(2), 863-1071.
12. Corey, J. Y. *Advances in Organometallic Chemistry*. Academic Press: San Diego, CA, 2004; pp. 1-52.
13. Lauterbur, P. C. *Determination of Organic Substances by Physical Methods*. Academic Press: New York, 1962; pp. 465-533.
14. Constantine, S. P.; Hitchcock, P. B.; Lawless, G. A. *Private Communication* **1995**.
15. Jutzi, P.; Kanne, D.; Hursthouse, M.; Howes, A. J. *Chem. Ber.* **1988,** 121, 1299-1305.
16. Jones, P. G.; Dix, I. *Private Communication* **2004**.

17. Hurkes, N.; Spirk, S.; Belaj, F.; Pietschnig, R. *Z. Anorg. Allg. Chem.* **2013,** 639(*14*), 2631-2636.
18. Blinka, T. A.; Helmer, B. J.; West, R. Polarization Transfer NMR Spectroscopy for Silicon-29: The INEPT and DEPT Techniques. In: F. G. A. Stone; W. Robert (Eds.), *Advances in Organometallic Chemistry*; Academic Press: San Diego, CA; 1984. p. 193-218.
19. Harloff, J.; Popowski, E.; Reinke, H. *J. Organomet. Chem.* **2007,** 692, 1421-1441.
20. Pink, H. S.; Kipping, F. S. *J. Chem. Soc. Trans.* **1923,** 123, 2830-2837.
21. Horvath, R. F.; Chan, T. H. *J. Org. Chem.* **1987,** 52, 4489-4494.
22. Chen, Y. X.; Rausch, M. D.; Chien, J. C. W. *Organometallics* **1993,** 12, 4607-4612.
23. Yamaguchi, S.; Akiyama, S.; Tamao, K. *Organometallics* **1998,** 17, 4347-4352.
24. Gilman, H.; Schwebke, G. L. *J. Org. Chem.* **1962,** 27(*12*), 4259-4261.
25. Grajewska, A.; Oestreich, M. *Synlett.* **2010,** 2010(*16*), 2482-2484.
26. Bent, H. A. *Chem. Rev.* **1961,** 61(*3*), 275-311.
27. Jennings, W. B.; Farrell, B. M.; Malone, J. F. *Acc. Chem. Res.* **2001,** 34(*11*), 885-894.
28. Meyer, E. A.; Castellano, R. K.; Diederich, F. *Angew. Chem., Int. Ed.* **2003,** 42(*11*), 1210-1250.
29. Janiak, C. *J. Chem. Soc., Dalton Trans.* **2000**, 3885-3896.
30. Zeppek, C.; Pichler, J.; Torvisco, A.; Flock, M.; Uhlig, F. *J. Organomet. Chem.* **2013,** 740, 41-49.
31. Zeppek, C.; Fischer, R. C.; Torvisco, A.; Uhlig, F. *Can. J. Chem.* **2014,** 92(*6*), 556-564.
32. Bernal, J. D. *Proc. R. Soc. London, Ser. A* **1924,** 106, 749-773.
33. Nakano, T.; Yade, T. *J. Am. Chem. Soc.* **2003,** 125(*50*), 15474-15484.
34. Cortial, G.; Le Goff, X.-F.; Bousquie, M.; Boisson, C.; Le Floch, P.; Nief, F.; Thuilliez, J. *New J. Chem.* **2010,** 34(*10*), 2290-2297.
35. Nemes, G. C.; Silaghi-Dumitrescu, L.; Silaghi-Dumitrescu, I.; Escudié, J.; Ranaivonjatovo, H.; Molloy, K. C.; Mahon, M. F.; Zukerman-Schpector, J. *Organometallics* **2005,** 24(*6*), 1134-1144.
36. Blessing, R. *Acta Cryst.* **1995,** 51(*1*), 33-38.
37. Sheldrick, G. M. *Acta Cryst.* **1990,** 46(*6*), 467-473.
38. Sheldrick, G. M. *Acta Cryst.* **2008,** 64(*1*), 112-122.
39. Spek, A. L. *J. Appl. Crystallogr.* **2003,** 36(*1*), 7-13.
40. Spek, A. L. *Acta Cryst.* **2009,** 65(*2*), 148-155.
41. Macrae, C. F.; Edgington, P. R.; McCabe, P.; Pidcock, E.; Shields, G. P.; Taylor, R.; Towler, M.; van de Streek, J. *J. Appl. Crystallogr.* **2006,** 39(*3*), 453-457.
42. Putz, H.; Brandenburg, K. *Diamond - Crystal and Molecular Structure Visualization. 3.2i.* Crystal Impact: Bonn.
43. Frisch, M. J.; Trucks, G. W.; Schlegel, H. B.; Scuseria, G. E.; Robb, M. A.; Cheeseman, J. R.; Scalmani, G.; Barone, V.; Mennucci, B.; Petersson, G. A.; Nakatsuji, H.; Caricato, M.; Li, X.; Hratchian, H. P.; Izmaylov, A. F.; Bloino, J.; Zheng, G.; Sonnenberg, J. L.; Hada, M.; Ehara, M.; Toyota, K.; Fukuda, R.; Hasegawa, J.; Ishida, M.; Nakajima, T.; Honda, Y.; Kitao, O.; Nakai, H.; Vreven, T.; Montgomery Jr., J. A.; Peralta, J. E.; Ogliaro, F.; Bearpark, M. J.; Heyd, J.; Brothers, E. N.; Kudin, K. N.; Staroverov, V. N.; Kobayashi, R.; Normand, J.; Raghavachari, K.; Rendell, A. P.; Burant, J. C.; Iyengar, S. S.; Tomasi, J.; Cossi, M.; Rega, N.; Millam, N. J.; Klene, M.; Knox, J. E.; Cross, J. B.; Bakken, V.; Adamo, C.; Jaramillo, J.; Gomperts, R.; Stratmann, R. E.; Yazyev, O.; Austin, A. J.; Cammi, R.; Pomelli, C.; Ochterski, J. W.; Martin, R. L.; Morokuma, K.; Zakrzewski, V. G.; Voth, G. A.; Salvador, P.; Dannenberg, J. J.; Dapprich, S.; Daniels, A. D.; Farkas, Ö.; Foresman, J. B.; Ortiz, J. V.; Cioslowski, J.; Fox, D. J. *Gaussian 09, Revision D.01.* Gaussian, Inc.: Wallingford, CT; 2013.
44. Adamo, C.; Barone, V. *J. Chem. Phys.* **1998,** 108, 664-675.
45. Zhao, Y.; Truhlar, D. G. *J. Chem. Phys.* **2006,** 125, 194101-194118.
46. Kutzelnigg, W.; Fleischer, U.; Schindler, M. *Deuterium and Shift Calculation*. Springer-Verlag: Berlin, **1991**; pp. 165-262.
47. Kuroda, K.; Ishikawa, N. *Nippon Kagaku Zasshi* **1969,** 90, 322-323.
48. Wiesinger, T. Novel cyclic arylsilanes, Master Thesis, TU Graz, Graz, **2013**.
49. Speck, S. B. *J. Org. Chem.* **1953,** 18, 1689-1700.
50. Ohshita, J.; Kimura, K.; Lee, K.-H.; Kunai, A.; Kwak, Y.-W.; Son, E.-C.; Kunugi, Y. *J. Polym. Sci., Part A: Polym. Chem.* **2007,** 45, 4588-4596.